IOP Conference Series: Earth and Environmental Science

PAPER • **OPEN ACCESS**

Cavitation CFD analyses considering the pressure wave propagation within the piping systems

To cite this article: Motohiko Nohmi *et al* 2019 *IOP Conf. Ser.: Earth Environ. Sci.* **240** 062025

View the article online for updates and enhancements.

This content was downloaded from IP address 159.226.140.26 on 08/10/2019 at 01:32

IOP Conf. Series: Earth and Environmental Science **240** (2019) 062025 doi:10.1088/1755-1315/240/6/062025

Cavitation CFD analyses considering the pressure wave propagation within the piping systems

Motohiko Nohmi[1], Shusaku Kagawa[2], Byungjin An[1], Tomoki Tsuneda[1], Kazuhiko Yokota[3] and Donghyuk Kang[4]

[1] EBARA Corporation, Fujisawa-shi, Japan
[2] EBARA Corporation, Futtsu-shi, Japan
[3] Aoyama Gakuin University, Sagamihara, Japan
[4] Saitama University, Saitama City, Japan

nohmi.motohiko@ebara.com

Abstract. Cavitation surge is a typical unsteady phenomenon and can be a cause of severe noise and vibration problems in hydraulic systems. When the oscillation frequency of the piping systems surrounding the hydraulic devices under cavitation surge is high and/or the pipe length is long, the acoustic wave propagation within the piping systems must be considered. In this study cavitation is computed by two dimensional CFD with cavitation model and the pressure wave in the piping systems is computed by one dimensional distributed model of Method Of Characteristics (MOC). The cavitation CFD and MOC calculations are coupled through boundary conditions. The interactions of cavitation and pressure wave are observed in the computed results.

1. Introduction

Cavitation surge is a typical unsteady cavitation phenomenon that is observed in many kinds of hydraulic devices such as contractions, hydrofoils, pumps and so on. The cavitation surge is characterized by the interaction of unsteady cavitation inside the flow passage and the piping system surrounding the passage. For computation of the cavitation surge, it is mandatory to consider the piping system dynamics. There are many attempts to compute the piping system dynamics with cavitating flow. Nohmi et al. computed the orifice flow with cavitation considering the piping system dynamics. Cavitating flow in the orifice tube is calculated by 2D-NS code and the flows inside the pipes are calculated by lumped parameter system analyses. The effects of pipe length on unsteady cavitation were also evaluated [1]. An et al. computed the incipient process of cavitation surge in the inducer blade cascade. The inlet boundary condition is coupled with unsteady Bernoulli equation considering the flow dynamics of the upstream pipe and tank [2]. Marie-Magdeleine et al. computed the cavitation in the Venturi pipe. 2D-NS code considering the compressibility of the liquid phase water is adopted. Flows inside the pipes are calculated by using Method Of Characteristics (MOC) [3]. Nanri et al. computed the acoustic cavitation surge of the turbopump with inlet pipe. The cavitation in the turbopump is computed by the lumped parameter system calculation utilizing cavitation compliance and mass flow gain factor. The flow in the inlet pipe is computed by MOC [4]. Present authors compared the computations of cavitation surge by using 3D-NS code and lumped parameter analyses concerning the piping system flow dynamics [5]. In

Content from this work may be used under the terms of the Creative Commons Attribution 3.0 licence. Any further distribution of this work must maintain attribution to the author(s) and the title of the work, journal citation and DOI.
Published under licence by IOP Publishing Ltd

the recent study by the present authors, the lumped parameter calculation and MOC calculation for upstream and downstream pipes of the cavitation surging pump are compared [6].

Table 1. Classification table of computation methods of pump cavitation surge with piping system dynamics.

			Piping System Calculation					
			Lumped Parameter System Calculation		**Distributed Parameter System Calculation**			
					One Dimensional Calcuation		**Two/Three Dimensional Calculation**	
			Incompressible Liquid Water	Compressible Liquid Water	Incompressible Liquid Water	Compressible Liquid Water	Incompressible Liquid Water	Compressible Liquid Water
Pump Calculation with Cavitataion	**Lumped Parameter System Calculation**	Incompressible Liquid Water	**5,6**			**4,6**		
		Compressible Liquid Water						
	Distributed Parameter System Calculation Two/Three Dimensional Calculation	Incompressible Liquid Water	**1,2,5**			**Present Study**		
		Compressible Liquid Water				**3**		

The computation methods of pump cavitation surge in time domain considering the dynamics of piping system are simply summarized in table 1 [6]. Numbers inside the table 1 are corresponding to references as written above. The computation of cavitation surge in frequency domain is also very beneficial, however if some transient phenomena and or irregular vibration are included, the unsteady dynamics of both cavitation and piping systems should be calculated correctly in time domain by using some methods in table 1.

From table 1 the most accurate method is computing the whole system by 3D-NS code considering the compressibility of the liquid phase water. However such expensive strategies cannot be practical at all under the limited CPU resources in industries. The first step to reduce computing time is to compute the system dynamics of the piping system not by 3D-NS code but by the lumped parameter system analyses or one dimensional distributed parameter calculation. When the compressibility of the liquid phase water inside the piping system ignored, the one dimensional analyses are just a calculation of unsteady Bernoulli equation and are equivalent to the lumped parameter system analysis. On the other hand, when the compressibility of the liquid phase water is concerned inside the piping system, the wave propagation in the pipes must be computed in the one dimensional analyses. For such computation, MOC would be the most popular methodology as aforementioned.

Although MOC requires much less CPU resources than 3D-NS computation, unnecessary computation of wave propagation should be avoided. The necessity of consideration of wave propagation in the pipe can be determined based on Ohashi-Akimoto criteria as seen in table 2 [6, 7, 8].

Table 2. Criterion for calculation method of piping system.

$L < k\frac{c}{f}$	Incompressible calculation is acceptable.
$L > k\frac{c}{f}$	Compressible calculation is needed.

where L is the pipe length, c is sound speed of the piping system, f is the characteristic frequency of the objective phenomenon and k is coefficient for criterion. Approximately 0.1 for k is recommended.

Lumped parameter model of cavitating flow is quite cost effective for computation. However, to build a model, identification of numerical values of cavitation compliance and mass flow gain factor is

necessary, and this is not easy. Rather it is straightforward to do 3D analysis with consideration of cavitation in today where computation cost is remarkably reduced.

In cavitating flow, the gas inside the cavitation bubbles is of course compressible. In so called cavitation CFD, the flow is calculated mostly by using the no slip mixture model of gas phase and liquid phase and the mixture medium in the discretized grids is compressible. On the other hand, it is controversial to treat the pure liquid phase surrounding the cavitating area as incompressible or compressible. Considering the compressibility of the liquid phase water would result in the accurate prediction however much more CPU time would also be required. In the most of the commercial CFD solvers, the liquid phase water surrounding cavitation is assumed incompressible.

2D/3D Cavitation CFD with the incompressible liquid phase assumption seems to have high affinity with the lumped parameter piping system analysis at first glance. However, there are difficulties in practice. 2D/3D Cavitation CFD and the lumped parameter piping system analysis are coupled through the boundary conditions. If the 2D/3D CFD and the lumped parameter calculation are explicitly coupled through static pressure prescribed boundary conditions, instability will occur in the computed system [1]. Implicit coupling may eliminate this instability, however the users of commercial CFD in industries does not have the source codes of the solver and cannot code the implicit calculations by using just a user subroutines.

In this research, another combination of 2D/3D Cavitation CFD with the incompressible liquid phase assumption and MOC for piping system calculations is tried and evaluated. As suggested in Ohashi-Akimoto criteria, the lumped parameter system calculation is only available for low frequency oscillation however MOC can be used in any frequency if there are enough grid points.

Further higher models include 2D/3D cavitation analysis considering liquid phase compressibility and MOC coupling. In this case, since the time increment of the 2D/3D analysis region is considerably smaller than the case where incompressibility is assumed from the Courant-Friedrichs-Lewy (CFL) condition, the calculation load increases. Therefore, if the pipe length is long and the time required for the wave propagation is large, the authors think that the method proposed in this research is more engineered and reasonable in many cases. The method of this study is described as Present Study in table 1.

2. Analytical object and computation method

The objective system is shown in figure 1. The typical flow system consists of a contraction passage, pipes with constant cross sectional area upstream and downstream of the contraction and tanks. At the contraction the velocity is increased and the static pressure is decreased and the cavitation occurs. This contraction is an exactly same model evaluated in the previous paper [1]. The flow in the contraction is assumed two dimensional. In this research, this cavitation flow was analyzed with the commercial code ANSYS-FLUENT. The cavitation is computed by using Schnerr-Sauer model, and the turbulence model is SST k-ω model. In the analysis of ANSYS-FLUENT, as described in chapter 1, non-cavitating water in the liquid phase in computation domain is treated as incompressible. To enhance cavitation unsteadiness, so called Reboud correction shown in equation (1) is used for the modification of turbulence model in cavitating area [10].

$$\mu_{t_{corrected}} = (\rho_l(1-\alpha)^n + \rho_v\alpha)\mu_t \tag{1}$$

where ρ_l is density of liquid water, ρ_v is density of vapor, α is void fraction, μ_t is eddy viscosity and n is the order of the exponential function. In this study, n is set to 5.

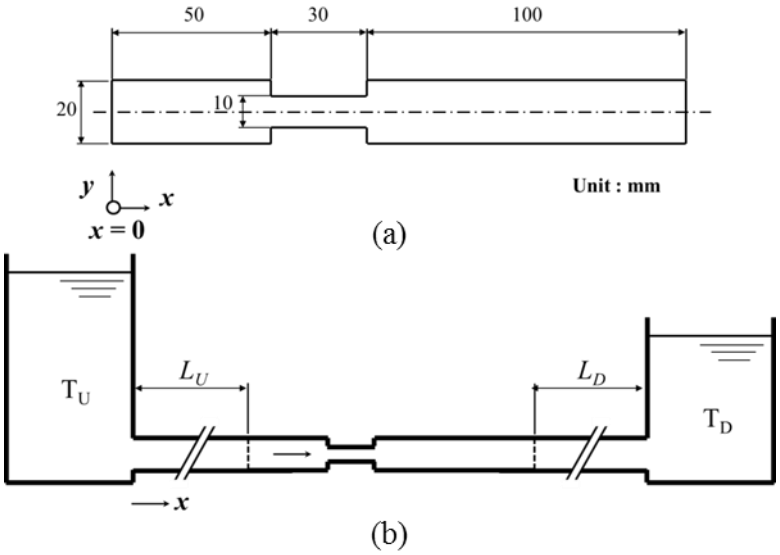

Figure 1. Objective contraction with piping system:
(a) objective contraction, (b) contraction with piping system.

The governing equations for one dimensional compressible distributed parameter system calculations for pipes are as follow.

$$\frac{\partial p}{\partial t} + \rho_l c^2 \frac{\partial u}{\partial x} = 0 \tag{2}$$

$$\frac{\partial u}{\partial t} + \frac{1}{\rho_l}\frac{\partial p}{\partial x} + \frac{\lambda}{D}\frac{|u|u}{2} = 0 \tag{3}$$

where x is axial location along the pipe, t is time, $p(x,t)$ and $u(x,t)$ are static pressure distribution and area averaged velocity distribution in the pipe, D is the diameter of the pipe and λ is Darcy's skin friction coefficient. Equation (2) and (3) are conservation equations of mass and momentum respectively. It is assumed that cavitation in the pipe, so called water column separation does not occur.

Boundary conditions at the tanks are simply as follow.

$$P_{TU}(t) = P_{CTU} \cdots\cdots\cdots const. \tag{4}$$

$$P_{TD}(t) = P_{CTD} \cdots\cdots\cdots const. \tag{5}$$

where P is static pressure, subscripts of TU and TD are the tank upstream the contraction and the tank downstream the contraction respectively. Subscripts of CTU and CTD are constant static pressure of the upstream tank and the downstream tank respectively.

Calculation parameters are as seen in table 3. It is assumed that the one dimensional sound speed c is less than the pure water sound speed because of the elastic deformation of the pipe. In this study c is set 1000 m/s or 900 m/s. In MOC calculation, weak compressibility is assumed and the value of ρ_l is constant.

Table 3. The calculation parameters.

Parameter	Value	Unit
D	0.02	m
L_U	1	m
L_D	1	m
ρ_l	998.2	kg/m^3
c	1000,900	m/s
λ	0.01	

Analysis of cavitation surge takes a long time, and this research focuses on shortening calculation time because it focuses on building robust analysis method. The two-dimensional computation domain is discretized with a uniform grid of Δx = 1 mm and Δy = 0.5 mm. The total number of grids is 6600, which is very coarse. Grid dependency evaluation was carried out by using fine grid of Δx = 0.5 mm and Δy = 0.25 mm for the case without MOC. Although slight difference was observed quantitatively, unsteady dynamic behaviors of cavitation showed good agreements in coarse grid case and fine grid case. The combination of fine grid and MOC is subject for the future.

Common time division of Δt is convenient for coupling of two-dimensional analysis region and one-dimensional MOC analysis region. Time division from preliminary two dimensional analyses is set to 5e-5 second. Axial grid size of Δx_{MOC} in MOC region is set to 5e-2 m from the CFL condition with c = 1000 m/s. Grid numbers for upstream and downstream pipes are 21 respectively.

The calculation procedure will be described in order as follows. The calculation is initially performed only in the two-dimensional region. Steady cavitation calculation with SST k-ω model is carried out. As the baseline boundary conditions, the velocity is fixed to 5 m/s at the inlet and the static pressure is fixed to 45000 Pa at the outlet. No-slip boundary is applied to the wall. The resultant flow field is used for the initial condition for the unsteady calculation in the next step.

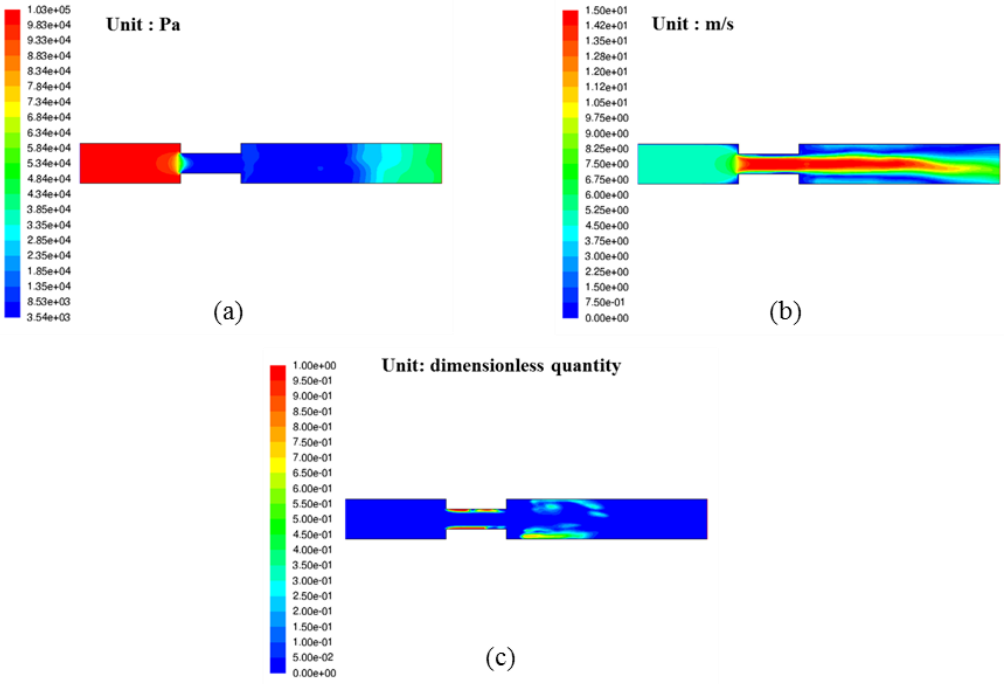

Figure 2. Instantaneous flow fields at t = 2.0 second:
(a) pressure distribution, (b) absolute velocity distribution, (c) void fraction.

Unsteady calculation with Reboud correction is carried out for 2 seconds until a stable cyclic variation is reached. Instantaneous flow fields at t = 2.0 second are shown in figure 2. It should be mentioned that the velocity field at the outlet of two-dimensional region is not uniform enough. The suitable position for the connection of two-dimensional and one-dimensional calculations should be in further study. This instantaneous flow field at t = 2.0 second is used for the initial condition for MOC coupled calculation. Assuming quasi steady flow, initial conditions for MOC region are as follow.

Upstream Pipe:

$$u(x,2) = u_{U2} \tag{6}$$

$$\frac{\partial p}{\partial x} = -\frac{\lambda}{2D}{u_{U2}}^2 \tag{7}$$

$$P_{CTU} = p_{U2} + \frac{\lambda L_U}{2D}{u_{U2}}^2 \tag{8}$$

Downstream Pipe:

$$u(x,2) = u_{D2} \tag{9}$$

$$\frac{\partial p}{\partial x} = -\frac{\lambda}{2D}{u_{D2}}^2 \tag{10}$$

$$P_{CTD} = p_{D2} - \frac{\lambda L_D}{2D}{u_{D2}}^2 \tag{11}$$

where subscripts *U2* and *D2* are inlet and outlet of two dimensional calculation region at t = 2 second respectively. From the boundary conditions u_{U2} is 5 m/s and p_{D2} is 45000 Pa. It should be mentioned that the instantaneous value of u_{D2} is not equal to u_{U2}.

Next, analysis that combines two-dimensional analysis and MOC is started. There is no precedent for analysis that sets the interface in the same kind of fluid, making one side compressible and the other side incompressible. First of all, the present authors attempted coupling under the Dirichlet condition that the flow velocity and static pressure coincide loosely at the boundary of both. The two-dimensional calculation and the MOC are explicitly coupled through each boundary condition as follows. In the two-dimensional calculation region, unsteady analysis is performed under the boundary conditions of the inlet flow velocity and the outlet static pressure, and the inlet average static pressure and the outlet average flow velocity obtained by the analysis are used as boundary conditions of the MOC. The boundary condition of the two-dimensional analysis region is updated using the inlet flow velocity and the outlet static pressure obtained by the MOC. The above process is repeated. When the test calculation was carried out, the calculation was unstable, and some stabilization measures were required. Therefore, in this research, the following two measures were carried out.

Firstly, an interpolation calculation was introduced into the MOC region, and the CFL number was lowered from 1 to 0.9. As a result, the sound speed was 900 m/s. The effect of relaxing vibration is added by interpolation calculation. Axial grid size of Δx_{MOC} in MOC region is kept 5e-2 m constant.

Secondly, in addition to the Dirichlet condition at the inlet part of the two-dimensional region, it also imposed the Neumann condition of zero velocity gradient.

Calculation was stabilized by the above processing.

In the actual phenomenon, when the pressure wave propagated in the pipe is incident on the cavitation region, part of the pressure wave is reflected and a part thereof is transmitted. On the other hand, in this study, the sound speed becomes infinite in the two-dimensional analysis region assuming incompressibility, but in the MOC region the sound speed becomes finite. Therefore, the acoustic impedance of both are extremely different, and reflection of the pressure wave occurs at the connecting portion between the both. It is desirable that the reflection at this connection in this study is similar to the reflection in the cavitation region of the real phenomenon. Whether the proposed method is valid or not is considered to be determined by the relationship between the time constant and the natural frequency of each incompressible two-dimensional analysis region and the MOC analysis region. The theoretical study will be a future subject.

3. Results and discussions

3.1. Unsteady results without MOC

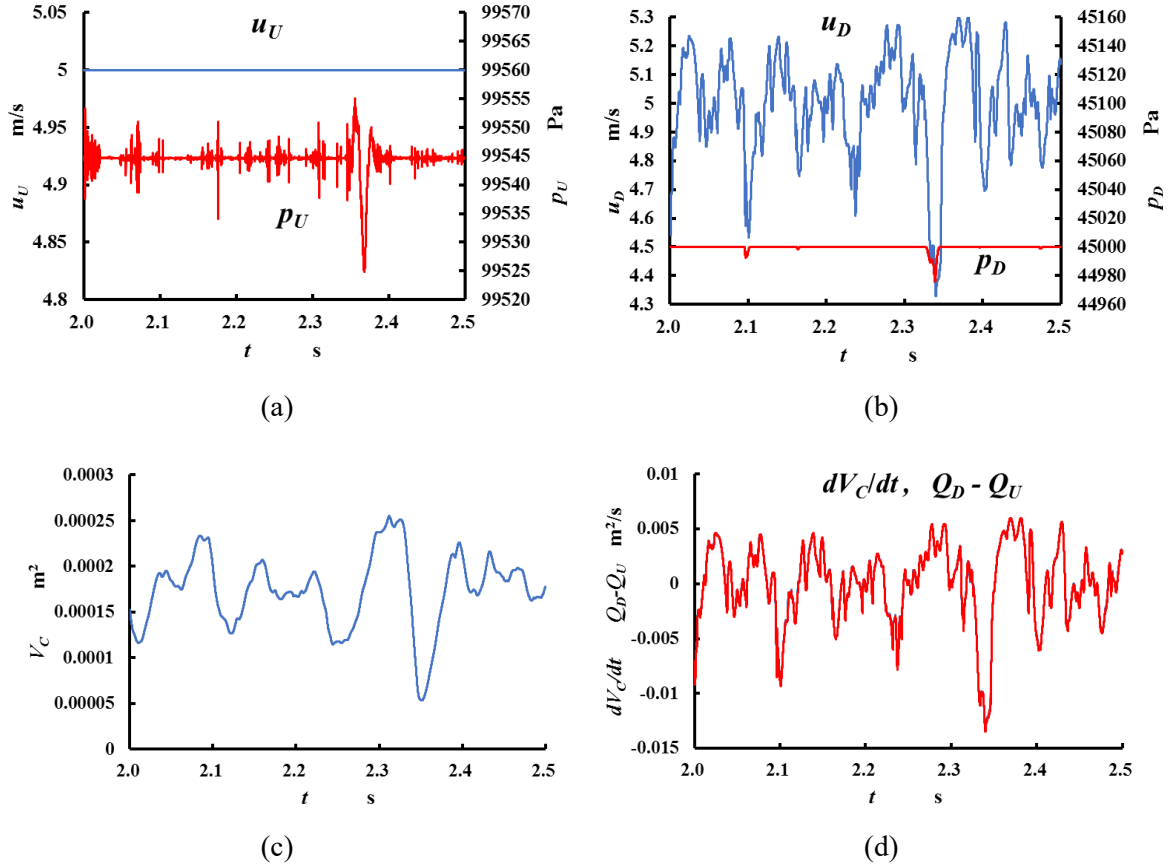

Figure 3. The unsteady results without MOC: (a) Velocity and static pressure at the inlet, (b) Velocity and static pressure at the outlet, (c) Cavitation volume, (d) Time derivative of cavitation volume and the difference of inlet and outlet volume flow rate.

For comparison, figure 3 shows the results of two-dimensional analysis without MOC extended by 0.5 seconds, where subscripts *U* and *D* are inlet and outlet of two dimensional calculation regions respectively. At the inlet, the velocity is kept constant. The static pressure shows some peaks, however

their amplitude are quite small. At the outlet the velocity fluctuates loosely periodically. Spectrum of the outlet velocity shows broadband peaks at around the frequency of 12 Hz from the FFT analysis.

The static pressure at the outlet is specified, however it shows some fluctuations. From the conservation of mass, it is expected that equation (12) is satisfied.

$$\frac{dV_c}{dt} = Q_D - Q_U \tag{12}$$

$$Q_U \equiv D \times u_U \tag{13}$$

$$Q_D \equiv D \times u_D \tag{14}$$

where V_C is the cavitation volume in the two-dimensional calculation region and Q is volume flow rate. It should be mentioned that the units of V_C and Q are m^2 and m^2/s respectively. In figure 3 (d), equation (12) is satisfied quite well.

3.2. Unsteady results with MOC

The unsteady calculation with MOC lasted until t = 2.1 second after the start but diverged afterwards. Figure 4 shows the contour maps of static pressure and mass flow rate on x-t planes. The static pressure on the center axis of the two-dimensional calculation region and MOC region is seen in figure 4 (a). The mass flow rate in each cross sections of the two-dimensional calculation region and MOC region is seen in figure 4 (b). The mass flow rate in MOC region is calculated simply from $\rho_l Du(x,t)$ and its unit is kg/ms. From figure 4 (a) reciprocation of the pressure wave is observed remarkably on the downstream of the two-dimensional calculation region. At around t = 2.09 s static pressure on the downstream decreases less than vapor pressure periodically. From figure 4 (b), mass flow fluctuations are seen on the downstream side of the contraction as with the pressure. On the other hand, on the upstream side, static pressure and mass flow fluctuate little. The reason for this may be due to intentional boundary condition settings of velocity specified at the inlet and static pressure specified at the outlet of the two-dimensional calculation region. Or due to the occurrence of cavitation, the speed of sound at the contraction becomes almost zero, chalking occurs, so the disturbance may not propagate upstream. More detailed analysis would be carried out in the future study.

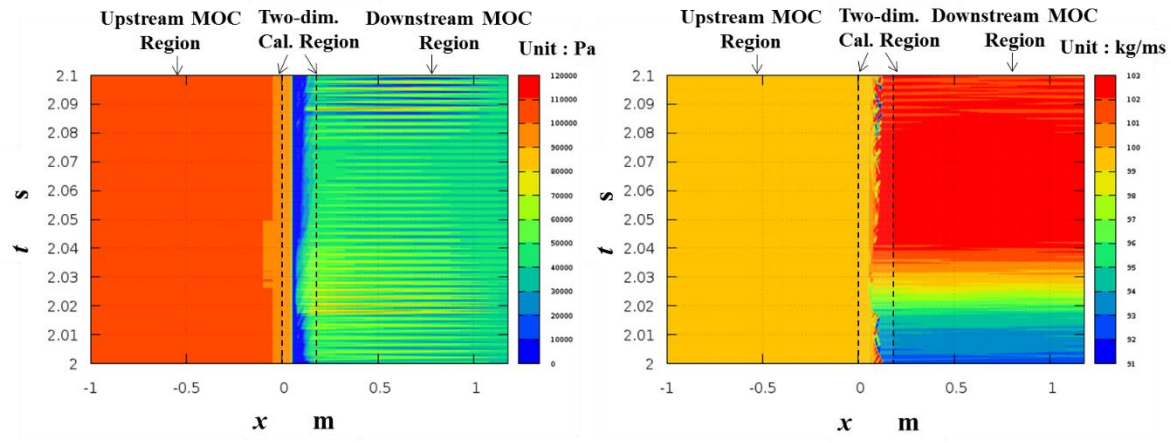

Figure 4. Contour maps of static pressure and mass flow rate along center axis on x-t planes: (a) static pressure distribution, (b) mass flow rate distribution.

The severe numerical vibration which causes the divergence of the calculation starts from around t = 2.08 s. Whether this indicates instability of numerical analysis simply or generation of acoustic resonance in piping system is also unknown at this stage. It is necessary to clarify these in the next stage.

Figure 5 shows static pressure and velocity at the inlet and outlet of the two-dimensional calculation region and the cavitation volume change from t = 2 s to t = 2.1 s. From figure 5 (b) it can be seen that the high frequency fluctuation is superimposed on the slow transient of the velocity change. The frequency of the fluctuation is 420 Hz from FFT analysis of u_D. This frequency is close to 450 Hz of $c/2L_D$, where c = 900 m/s. The slight difference of 420 Hz and 450 Hz may be due to the additional compliance of cavitation [9]. The change of the static pressure and the velocity at the inlet are much weaker than those at the outlet. From figure 5 (d), equation (12) is still satisfied quite well. These results suggest that the analytical method proposed in this research may have capabilities for both analysis of inertial cavitation surge and analysis of acoustic cavitation surge [6, 9]. It should be noted that it is necessary to add a function to consider water column separation in MOC analysis in order to analyze the acoustic cavitation surge [4].

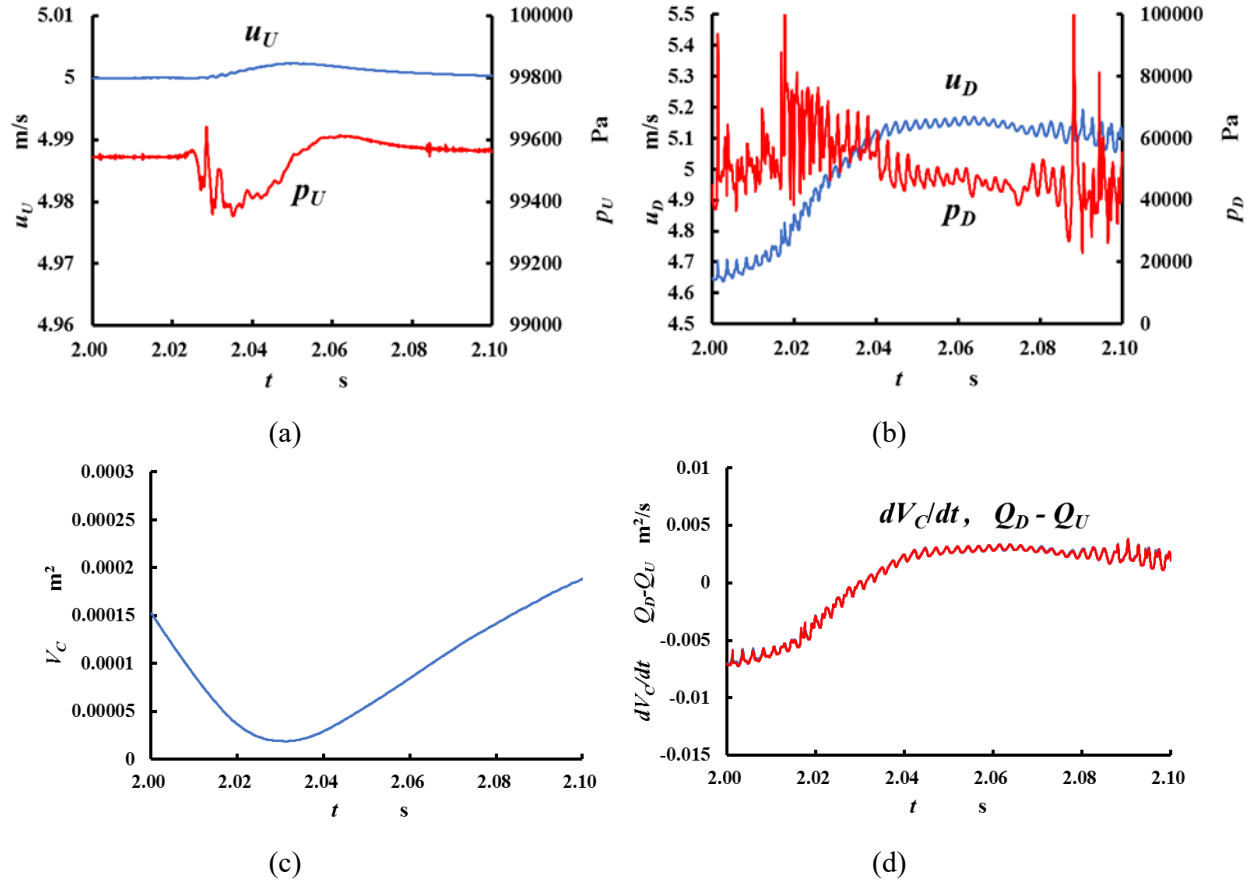

Figure 5. The unsteady results with MOC: (a) velocity and static pressure at the inlet, (b) velocity and static pressure at the outlet, (c) cavitation volume, (d) time derivative of cavitation volume and the difference of inlet and outlet volume flow rate.

4. Concluding remarks

The cavitation surge is characterized by the interaction of unsteady cavitation inside the flow passage and the piping system surrounding the passage. For computation of the cavitation surge, it is mandatory to consider the piping system dynamics. In this study cavitation is computed by two dimensional CFD

with cavitation model and the pressure wave in the piping systems is computed by one dimensional distributed model of Method Of Characteristics (MOC). Coupled analysis of the unsteady behavior of cavitation and the propagation of the pressure wave in the pipe is proved to be possible. The dynamics of unsteady cavitation is totally different depending on the presence or absence of the pressure wave propagation in the piping system. Although the proposed analysis method still has stability issues, it will be possible to further understand the cavitation surge phenomenon by using this analysis method.

Acknowledgement
The authors would like to express their sincere thanks to Mr. Naoki Kodama for his significant contribution to the complicated CFD works.

Appendices
The latest results those are much stabilized by reduction of CFL number to 0.5 are seen in figure 6. In this condition, sound speed of the piping system is 500 m/s. Calculation can be carried out stably up to 3 seconds. After transient period, the system looks reaching the periodically fluctuating state of the frequency of about 4 Hz.

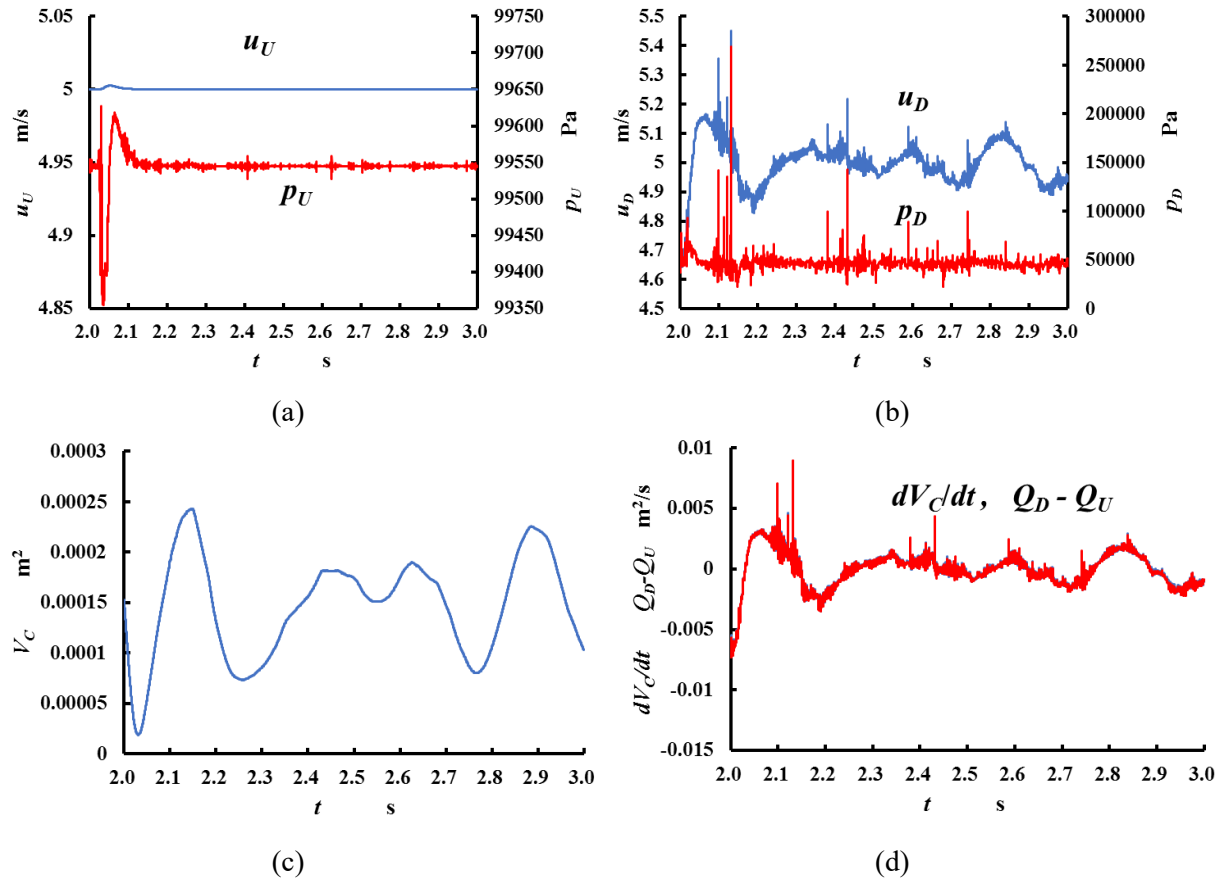

Figure 6. The unsteady results with MOC (CFL number is 0.5): (a) velocity and static pressure at the inlet, (b) velocity and static pressure at the outlet, (c) cavitation volume, (d) time derivative of cavitation volume and the difference of inlet and outlet volume flow rate.

References
[1] Nohmi M, Ikohagi T and Iga Y 2011 On boundary conditions for cavitation CFD and system dynamics of closed loop channel AJK2011-33007
[2] An B and Kajishima T 2013 Transition from rotating cavitation to cavitation surge in a two-

dimensional cascade *JSME Journal of Fluid Science and Technology* **8(1)** pp 20-29
[3] Marie-Magdeleine A, Fortes-Patella R, Lemoine N and Marchand N 2012 Unsteady flow rate simulations methodology for identification of the dynamic transfer function of a cavitating Venturi *Proc. CAV2012* pp 527-533
[4] Nanri H, Fujiwara T, Kannan H and Yoshida Y 2011 One-dimensional analysis of cavitation surge considering the acoustic effect of the inlet line in a rocket engine turbopump (3rd report, Discontinuity of oscillating frequency caused by nonlinear factors) *Transaction of the Japan Society of Mechanical Engineers Series B* **77(780)** pp 1630-1640 in Japanese
[5] Nohmi M, Yamazaki S, Kagawa S, An B, Kang D and Yokota K 2016 Numerical analyses for cavitation surge in a pump with the square root shaped suction performance curve ISROMAC-2016
[6] Nohmi M, Yamazaki S, Kagawa S, An B, Kang D and Yokota K 2017 Numerical study of one dimensional pipe flow under pump cavitation surge FEDSM2017-69427
[7] Nohmi M, Yamazaki S, Kagawa S, An B, Kang D and Yokota K 2016 Numerical study of ohashi's criterion *the 18th Symposium for Cavitation in Japan* in Japanese
[8] Nohmi M, Yamazaki S, Kagawa S, An B, Kang D and Yokota K 2018 Numerical study of criteria proposed by ohashi and akimoto First report: A case study of a simple hydraulic oscillating system *Ebara Engineering Review* **255** pp 19-23 in Japanese
[9] Nanri H, Kannan H, Tani N and Yoshida Y 2010 Analysis of acoustic cavitation surge in a rocket engine turbopump *International Journal of Rotating Machinery* **2010** Article ID 717013
[10] Coutier-Delgosha O, Fortes-Patella R and Reboud J L 2003 Evaluation of turbulence model influence on the numerical simulations of unsteady cavitation *J. Fluids Eng.* **125(1)** pp 38-45